Journal of Macromolecular Science, Part A
Publication details, including instructions for authors and subscription information:
http://www.informaworld.com/smpp/title~content=t713597274

Liquid—Liquid Equilibrium in Polydisperse Random Copolymer Blends

Margit T. Rätzsch[a]; Christian Wohlfarth[a]; Dieter Browarzik[a]; Horst Kehlen[a]
[a] Department of Chemistry, "Carl Schorlemmer" Technical University, Merseburg, German Democratic Republic

To cite this Article Rätzsch, Margit T. , Wohlfarth, Christian , Browarzik, Dieter and Kehlen, Horst(1989) 'Liquid—Liquid Equilibrium in Polydisperse Random Copolymer Blends', Journal of Macromolecular Science, Part A, 26: 11, 1497 — 1523
To link to this Article: DOI: 10.1080/00222338908052068
URL: http://dx.doi.org/10.1080/00222338908052068

J. MACROMOL. SCI.–CHEM., A26(11), pp. 1497-1523 (1989)

LIQUID–LIQUID EQUILIBRIUM IN POLYDISPERSE RANDOM COPOLYMER BLENDS

MARGIT T. RÄTZSCH,* CHRISTIAN WOHLFARTH,
DIETER BROWARZIK, and HORST KEHLEN

Department of Chemistry
"Carl Schorlemmer" Technical University
DDR-4200 Merseburg, German Democratic Republic

ABSTRACT

Continuous thermodynamics is applied to the liquid-liquid equilibrium in random copolymer blends. Two copolymers are mixed, each consisting of two different monomer units. Hence, up to four monomer units may be present in the system. Both copolymers are characterized by divariate distribution functions with respect to molecular weight (chain length) and chemical composition. The basic relations necessary for phase equilibrium calculations are derived. The influences of both polydispersities and of the different parameters included in the model for the excess Gibbs free energy are discussed by calculating cloud-point curves and shadow curves. Applications to practical systems are given.

INTRODUCTION

The problem of compatibility in copolymer blends has long been a subject of interest. Dating back to the first beginnings in the 1940s, a large number of papers on this subject has appeared. However, the great majority of these studies deal with practical aspects in regard to certain industrial purposes, and only relatively few studies are related to the basic thermodynamics of compatibility. Roe and Rigby [1] have recently reviewed the state of art in this field. Probably the most striking feature of copolymer blends is that

miscibility may occur even in the absence of any specific interactions between their monomer units if the repulsive interactions are sufficiently strong [2, 3]. Attempts to describe demixing phenomena in systems with copolymers started with the pioneering paper by Scott [4], which used the solubility parameter concept.

Recent approaches use free-volume models [5, 6] or lattice models [2, 3, 7-9] to explain certain experimental findings, but in most cases (e.g., Refs. 2-9 and further papers cited in Ref. 1) there was no calculation of the complete phase diagrams, and only Koningsveld et al. [7, 9] took the polydispersity of the copolymers into account. Furthermore, the thermodynamic considerations were usually restricted to an analysis of the spinodal and/or the critical state criterion or even more qualitatively to the negative sign of the Gibbs free energy of mixing only.

The calculation of phase diagrams in multicomponent systems is commonly considered to be a tedious task. However, continuous thermodynamics provides an elegant solution of this problem [10-12] which also holds true for solutions containing copolymers characterized by divariate distribution functions [13-15]. A first attempt was also made for a homopolymer/copolymer blend [16].

Continuous thermodynamics will be applied in this paper to blends of two random copolymers, each consisting of two different monomer units and both characterized by divariate distribution functions. The influences of both chemical and molecular weight distributions and of the different parameters included in the thermodynamic model describing the activity coefficients on the liquid-liquid equilibrium are discussed.

DIVARIATE DISTRIBUTION FUNCTIONS

Copolymers B and C are considered to each consist of two kinds of monomer units, α and β in B, γ and δ in C. Choosing a standard segment of arbitrary size, the segment numbers r_α, r_β, r_γ, and r_δ can be introduced. The total segment numbers r_B and r_C and the segment fractions Y_B and Y_C of the α and the γ monomer units within the molecules are given by

$$r_B = r_\alpha + r_\beta, \quad Y_B = r_\alpha / r_B;$$
$$r_C = r_\gamma + r_\delta, \quad Y_C = r_\gamma / r_C. \tag{1}$$

Then the compositions of the polydisperse copolymers may be described by the divariate distribution functions $W_B(r_B, Y_B)$ and $W_C(r_C, Y_C)$, neglecting other polydispersities (e.g., sequence distribution, branching, etc.). These divariate distribution functions have to fulfill the normalization condition

$$\int_{r_B}\int_{Y_B} W_B(r_B, Y_B)\, dY_B\, dr_B = 1; \quad \int_{r_B} = \int_{r_0}^{r^0}; \quad \int_{Y_B} = \int_0^1, \tag{2}$$

which holds true for Copolymer C, too.

The number-average $\bar{r}$ and the (weight) segment average $\tilde{r}$ of the segment number as well as the weight average $\tilde{Y}$ of the chemical distribution are defined by

$$\frac{1}{\bar{r}_B} = \int_{r_B}\int_{Y_B} W_B(r_B, Y_B)\frac{1}{r_B}\, dY_B\, dr_B \tag{3a}$$

$$\tilde{r}_B = \int_{r_B}\int_{Y_B} W_B(r_B, Y_B) r_B\, dY_B\, dr_B \tag{3b}$$

$$\tilde{Y}_B = \int_{r_B}\int_{Y_B} W_B(r_B, Y_B) Y_B\, dY_B\, dr_B \tag{3c}$$

The corresponding equations for Copolymer C are obtained by replacing the index B by C.

For the sake of simplicity with respect to the mathematical problems involved with the double integrals, Copolymers B and C are assumed to obey (as random products) the generalized Stockmayer distribution as used in our earlier papers on copolymer solutions [13-15].

$$W_B(r_B, Y_B) = \left\{ \frac{k_B{}^{k_B+1}}{\bar{r}_B \Gamma(k_B+1)} \left(\frac{r_B}{\bar{r}_B}\right)^{k_B} \exp\left(-k_B \frac{r_B}{\bar{r}_B}\right) \right\} \left\{ \frac{r_B}{2\pi\epsilon_B} \exp\left(-\frac{r_B(Y_B - \tilde{Y}_B)^2}{2\epsilon_B}\right) \right\} \tag{4}$$

where Γ is the gamma function, and k_B and ϵ_B are given by

$$k_B = 1/(\tilde{r}_B/\bar{r}_B - 1), \tag{5a}$$

$$\epsilon_B = \tilde{Y}_B(1 - \tilde{Y}_B). \tag{5b}$$

The equations for C again read like those for B but with index C instead of B.

PHASE EQUILIBRIUM BY CONTINUOUS THERMODYNAMICS

The conditions for phase equilibrium are formulated on the basis of chemical potentials. For a mixture containing Copolymers B and C, the equilibrium condition reads [13]

$$\mu_B'(r_B, Y_B) = \mu_B''(r_B, Y_B), \tag{6a}$$

$$\mu_C'(r_C, Y_C) = \mu_C''(r_C, Y_C), \tag{6b}$$

i.e., the chemical potential $\mu_i(r_i, Y_i)$ is equal in both phases $'$ and $''$ for all species identified by segment numbers r_B and r_C and by chemical compositions Y_B and Y_C, respectively. With the Flory-Huggins mixture as the reference state, the chemical potentials read [13]

$$\mu_B(r_B, Y_B) = \mu^*_{B,0}(r_B, Y_B) + RT[\ln \psi_B W_B(r_B, Y_B) + 1 - r_B/\bar{r}] + r_B RT \ln \bar{\bar{f}}_B(r_B, Y_B), \tag{7a}$$

$$\mu_C(r_C, Y_C) = \mu^*_{C,0}(r_C, Y_C) + RT[\ln \psi_C W_C(r_C, Y_C) + 1 - r_C/\bar{r}] + r_C RT \ln \bar{\bar{f}}_C(r_C, Y_C), \tag{7b}$$

where R is the universal gas constant, T is the absolute temperature, and $\bar{r}$ is defined by

$$\frac{1}{\bar{r}} = \frac{\psi_B}{\bar{r}_B} + \frac{\psi_C}{\bar{r}_C}, \tag{8}$$

where $\bar{r}_B$ and $\bar{r}_C$ are given by Eq. (3a). The chemical potentials $\mu^*_{B,0}$ and $\mu^*_{C,0}$ contain contributions due to the pure species (which do not influence

the phase equilibrium calculation). The quantities $\bar{\bar{f}}_B$ and $\bar{\bar{f}}_C$ are the so-called segment-molar activity coefficients containing all deviations from the Flory-Huggins mixture. The phase-equilibrium conditions, Eq. (6), lead to

$$\psi_B'' W_B''(r_B, Y_B) = \psi_B' W_B'(r_B, Y_B) \exp(r_B \rho_B(r_B, Y_B)), \tag{9a}$$

$$\psi_C'' W_C''(r_C, Y_C) = \psi_C' W_C'(r_C, Y_C) \exp(r_C \rho_C(r_C, Y_C)), \tag{9b}$$

where

$$\rho_B = \ln(\bar{\bar{f}}_B'/\bar{\bar{f}}_B'') + 1/\bar{r}'' - 1/\bar{r}', \tag{9c}$$

$$\rho_C = \ln(\bar{\bar{f}}_C'/\bar{\bar{f}}_C'') + 1/\bar{r}'' - 1/\bar{r}'. \tag{9d}$$

Further treatment depends on how the distribution functions $W_B(r_B, Y_B)$ and $W_C(r_C, Y_C)$ influence the segment-molar activity coefficients $\bar{\bar{f}}_B$ and $\bar{\bar{f}}_C$. The logarithms of $\bar{\bar{f}}_B$ and $\bar{\bar{f}}_C$ are the partial segment-molar quantities with respect to the segment-molar excess Gibbs energy, $\bar{\bar{G}}^E/RT$. Here, excess means the deviation from the Flory-Huggins mixture.

$\bar{\bar{G}}^E$-MODEL AND ACTIVITY COEFFICIENTS

Explicit expressions have to be developed for the segment-molar activity coefficients in the equations discussed above in order to perform numerical calculations. By using the random mixing assumption for all kinds of segments and applying the continuous description of the mixture, we obtain the number of all α-contacts (equal to the probability of all α-contacts) per mole of segments of the mixture B + C:

$$\begin{aligned}\bar{\bar{A}}_\alpha &= 2\bar{\bar{A}}_{\alpha\alpha} + \bar{\bar{A}}_{\alpha\beta} + \bar{\bar{A}}_{\alpha\gamma} + \bar{\bar{A}}_{\alpha\delta} \\ &= s_\alpha \psi_B \int_{r_B} \int_{Y_B} W_B(r_B, Y_B) Y_B \, dY_B \, dr_B \\ &= s_\alpha \psi_B \tilde{Y}_B. \end{aligned} \tag{10a}$$

Here $\bar{\bar{A}}_{\alpha\alpha}$, $\bar{\bar{A}}_{\alpha\beta}$,. . . are the numbers of contacts specified. The relations

$$\bar{\bar{A}}_{\beta} = s_\beta \psi_B (1 - \tilde{Y}_B); \quad \bar{\bar{A}}_{\gamma} = s_\gamma \psi_C \tilde{Y}_C; \quad \bar{\bar{A}}_{\delta} = s_\delta \psi_C (1 - \tilde{Y}_C) \tag{10b}$$

are obtained in an analogous way. The quantities ψ_B and ψ_C are the overall segment fractions of all copolymer species B and C, respectively. The quantities s_i ($i = \alpha, \beta, \gamma, \delta$) are surface-contact numbers. Random mixing is provided by the surface contact probability

$$\begin{aligned}
\bar{\bar{A}}_{\alpha\beta} &= s_\alpha \tilde{Y}_B \psi_B \theta_\alpha = s_\beta (1 - \tilde{Y}_B) \psi_B \theta_\alpha = \bar{\bar{A}}_{\beta\alpha} \\
\bar{\bar{A}}_{\alpha\gamma} &= s_\alpha \tilde{Y}_B \psi_B \theta_\gamma s_\gamma \tilde{Y}_C \psi_C \theta_\alpha \qquad = \bar{\bar{A}}_{\gamma\delta} \\
&\vdots \qquad\quad \vdots \qquad\qquad\qquad \vdots \\
&\ldots
\end{aligned} \tag{11}$$

where the surface fractions θ_i ($i = \alpha, \beta, \gamma, \delta$) are defined by

$$\begin{aligned}
&\theta_\alpha = s_\alpha \tilde{Y}_B \psi_B / Q; \quad \theta_\beta = s_\beta (1 - \tilde{Y}_B) \psi_B / Q; \\
&\theta_\gamma = s_\gamma \tilde{Y}_C \psi_C / Q; \quad \theta_\delta = s_\delta (1 - \tilde{Y}_C) \psi_C / Q; \\
&Q = \eta_1 \psi_B + \eta_2 \psi_C; \\
&\eta_1 = s_\alpha \tilde{Y}_B + s_\beta (1 - \tilde{Y}_B); \quad \eta_2 = s_\gamma \tilde{Y}_C + s_\delta (1 - \tilde{Y}_C).
\end{aligned} \tag{12}$$

The segment molar internal energy of mixing, $\Delta_M \bar{\bar{U}}$, can be obtained the usual way by addition of all contributions $\bar{\bar{A}}_{ij} U_{ij}$ and subtraction of the terms already present in the pure Copolymers B or C. The final result reads

$$\begin{aligned}
\Delta_M \bar{\bar{U}} = \frac{\psi_B \psi_C}{Q} \Bigg[& -s_\alpha s_\beta \tilde{Y}_B (1 - \tilde{Y}_B) \frac{\eta_2}{\eta_1} \Delta U_{\alpha\beta} + s_\alpha s_\gamma \tilde{Y}_B \tilde{Y}_C \Delta U_{\alpha\gamma} \\
& + s_\alpha s_\delta \tilde{Y}_B (1 - \tilde{Y}_C) \Delta U_{\alpha\delta} + s_\beta s_\gamma (1 - \tilde{Y}_B) \tilde{Y}_C \Delta U_{\beta\gamma} \\
& + s_\beta s_\delta (1 - \tilde{Y}_B)(1 - \tilde{Y}_C) \Delta U_{\beta\delta} - s_\gamma s_\delta \tilde{Y}_C (1 - \tilde{Y}_C) \frac{\eta_1}{\eta_2} \Delta U_{\gamma\delta} \Bigg].
\end{aligned} \tag{13}$$

The quantities ΔU_{ij} are differences of interaction energies of the type

$$\Delta U_{ij} = U_{ij} - \frac{1}{2}(U_{ii} + U_{jj}); \quad i,j = \alpha, \beta, \gamma, \delta. \tag{14}$$

As usual in polymer solution, thermodynamics interaction parameters of the type

$$g_{ij} = s_0 \Delta U_{ij}/RT \tag{15}$$

may be introduced, in which s_0 is a standard surface area (which may be equal to s_α).

To simplify computations, all g_{ij} parameters are assumed to depend in a uniform way on T, i.e., by the common function $\beta(T)$, so that $g_{ij} = g_{ij}\beta(T)$. The pressure dependence is neglected in this paper. Furthermore, a modified concentration-dependent prefactor $L(\psi_B)$ is used in $\bar{\bar{G}}^E$ instead of $\psi_B\psi_C$. only. Finally, these considerations result in an expression for $\bar{\bar{G}}^E$ of the type

$$\frac{\bar{\bar{G}}^E}{RT} = \frac{L(\psi_B)}{Q}\beta(T)g, \tag{16}$$

with

$$L(\psi_B) = \psi_B(1 - \psi_B)(1 + c\psi_B + d\psi_B{}^2). \tag{17}$$

Here g results from the terms in the brackets of Eq. (13), expressing the quantities ΔU_{ij} via Eq. (15) and $g_{ij} = g_{ij}\beta(T)$ by the parameters g_{ij}.

The function $\beta(T)$ is assumed to follow

$$\beta(T) = a + b/T. \tag{18}$$

It is important to note that $\beta(T)$ (and not the g_{ij} parameters) includes the weighting factors accounting for the choices of the size of the standard segment and of the standard surface area. If we confine ourselves to mixtures of copolymers of the same type, i.e., B($\alpha\beta$) + C($\alpha\beta$), and use $c = d = 0$ in $L(\psi_B)$, Eq. (16) for $\bar{\bar{G}}^E/RT$ reduces to the result published by Koningsveld et al. [7-9], and if we assume additionally $s_i = 1$, $i = \alpha,\beta$, it becomes the equation discussed by Scott [4]. With neglect of polydispersity and use again of $c = d = 0$, and all $s_i = 1$, Eq. (16) reduces to the relation given recently by dif-

ferent authors (e.g., Refs. 1-3) in their discussion of miscibility behavior in monodisperse copolymer mixtures. There is also agreement with our relations used recently for copolymer solutions in the polydisperse case [14, 15].

The segment-molar activity coefficients are derived according to the methods outlined elsewhere [13]. As $\bar{\bar{G}}^E$ depends on the weight-averages $\tilde{Y}_B$ and $\tilde{Y}_C$ the activity coefficients depend on Y_B and Y_C, respectively, but not on r_B or r_C.

$$\ln \bar{\bar{f}}_B(Y_B) = \frac{\bar{\bar{G}}^E}{RT} + (1 - \psi_B)\frac{\partial \bar{\bar{G}}^E/RT}{\partial \psi_B} + \frac{1}{\psi_B}\frac{\partial \bar{\bar{G}}^E/RT}{\partial \tilde{Y}_B}(Y_B - \tilde{Y}_B), \tag{19a}$$

$$\ln \bar{\bar{f}}_C(Y_C) = \frac{\bar{\bar{G}}^E}{RT} - \psi_B\frac{\bar{\bar{G}}^E/RT}{\partial \psi_B} + \frac{1}{1 - \psi_B}\frac{\partial \bar{\bar{G}}^E/RT}{\partial \tilde{Y}_C}(Y_C - \tilde{Y}_C), \tag{19b}$$

where

$$\frac{\partial \bar{\bar{G}}^E/RT}{\partial \psi_B} = \frac{g}{Q^2}(QL_x - LQ_x)\beta(T), \tag{20}$$

with

$$L_x = 1 + 2(c - 1)\psi_B + 3(d - c)\psi_B{}^2 - 4d\psi_B{}^3, \tag{21}$$

$$Q_x = \eta_1 - \eta_2, \tag{22}$$

and

$$\frac{\partial \bar{\bar{G}}^E/RT}{\partial \tilde{Y}_B} = \frac{L}{Q}\left[\frac{\partial g}{\partial \tilde{Y}_B} - \frac{g}{Q}\psi_B(s_\alpha - s\beta)\right]\beta(T), \tag{23a}$$

$$\frac{\partial \bar{\bar{G}}^E/RT}{\partial \tilde{Y}_C} = \frac{L}{Q}\left[\frac{\partial g}{\partial \tilde{Y}_C} - \frac{g}{Q}(1 - \psi_B)(s_\gamma - s_\delta)\right]\beta(T), \tag{23b}$$

$$\frac{\partial g}{\partial \tilde{Y}_B} = s_\alpha s\beta\frac{\eta_2}{\eta_1{}^2}g_{\alpha\beta}[s_\alpha \tilde{Y}_B{}^2 - s\beta(1 - \tilde{Y}_B)^2] + s_\alpha s_\gamma \tilde{Y}_C g_{\alpha\gamma} + s_\alpha s_\delta(1 - \tilde{Y}_C)g_{\alpha\delta}$$

$$- s\beta s_\gamma \tilde{Y}_C g_{\beta\gamma} - s\beta s_\delta(1 - \tilde{Y}_C)g_{\beta\delta} - \frac{s_\gamma s_\delta}{\eta_2}\tilde{Y}_C(1 - \tilde{Y}_C)(s_\alpha - s\beta)g_{\gamma\delta}, \tag{24a}$$

$$\frac{\partial g}{\partial \tilde{Y}_C} = -\frac{s_\alpha s_\beta}{\eta_1}\tilde{Y}_B(1-\tilde{Y}_B)(s_\gamma - s_\delta)g_{\alpha\beta} + s_\alpha s_\gamma \tilde{Y}_B g_{\alpha\gamma} + s_\beta s_\gamma (1-\tilde{Y}_B)g_{\beta\gamma}$$

$$- s_\alpha s_\delta \tilde{Y}_B g_{\alpha\delta} - s_\beta s_\delta (1-\tilde{Y}_B)g_{\beta\delta} + s_\gamma s_\delta \frac{\eta_1}{\eta_2^2} g_{\gamma\delta}[s_\gamma \tilde{Y}_C^2 - s_\delta(1-\tilde{Y}_C)^2]. \tag{24b}$$

CLOUD-POINT CURVE AND SHADOW CURVE

In this paper, consideration will be restricted to the boundary curves describing the beginning of phase separation in polydisperse mixtures, i.e., the temperature of a given phase ′ is changed at constant pressure until "the first droplet" of the second phase ″ is formed. The plot of the equilibrium temperature T versus ψ_B' is called the cloud-point curve and the plot of T versus ψ_B'' is called the shadow curve. Thus, the unknowns are T, ψ_B'', and the distribution functions $W_B''(r_B, Y_B)$ and $W_C''(r_C, Y_C)$. The solution of this problem is performed in a manner analogous to that described in earlier papers [10-12]. Equations (9a-b) and (3a-c) lead to the unknown scalars of the problem. For Copolymer B, the equations read

$$\psi_B'' = \psi_B' \int_{r_B}\int_{Y_B} W_B'(r_B, Y_B) \exp(r_B \rho_B(r_B, Y_B))\, dY_B\, dr_B, \tag{25a}$$

$$\frac{1}{\bar{r}_B''} = \frac{\psi_B'}{\psi_B''} \int_{r_B}\int_{Y_B} W_B'(r_B, Y_B) \exp(r_B \rho_B(r_B, Y_B)) \frac{1}{r_B} dY_B\, dr_B, \tag{25b}$$

$$\tilde{Y}_B'' = \frac{\psi_B'}{\psi_B''} \int_{r_B}\int_{Y_B} W_B'(r_B, Y_B) \exp(r_B \rho_B(r_B, Y_B)) Y_B\, dY_B\, dr_B. \tag{25c}$$

Replacement of the index B by C leads to the relations for the unknown scalars of Copolymer C. All double integrals can be solved analytically when the generalized Stockmayer distribution function, Eq. (4), is applied for $W_B'(r_B, Y_B)$ and $W_C'(r_C, Y_C)$. As in the case of copolymer solutions (solvent A + polydisperse copolymer B) [13, 14], both distribution functions $W_B''(r_B, Y_B)$ and $W_C''(r_C, Y_C)$ of the shadow phase are again generalized Stockmayer distributions possessing the same values k_B, ϵ_B and k_C, ϵ_C, respectively, of the parent distribution functions in the homogeneous phase ′. The solution of the double integrals in Eqs. (25a-c) then provides the following relations:

$$\bar{r}_B'' = \bar{r}_B' \left(\frac{\psi_B''}{\psi_B'} \right)^{1/(k_B+1)}, \tag{26a}$$

$$\bar{r}_C'' = \bar{r}_C' \left(\frac{\psi_C''}{\psi_C'} \right)^{1/(k_C+1)}, \tag{26b}$$

$$\psi_B'' = \psi_B' / [1 - (\bar{r}_B'/k_B)(A_B + B_B \tilde{Y}_B' + \epsilon_B B_B^2/2)]^{k_B+1}, \tag{27a}$$

$$\psi_C'' = \psi_C' / [1 - (\bar{r}_C'/k_C)(A_C + B_C \tilde{Y}_C' + \epsilon_C B_C^2/2)]^{k_C+1}, \tag{27b}$$

$$\tilde{Y}_B'' = \tilde{Y}_B' + \epsilon_B B_B, \tag{28a}$$

$$\tilde{Y}_C'' = \tilde{Y}_C' + \epsilon_C B_C. \tag{28b}$$

The functions A_B, B_B, A_C, and B_C are defined by

$$\rho_B = A_B + B_B Y_B, \tag{29a}$$

$$\rho_C = A_C + B_C Y_C, \tag{29b}$$

where

$$A_B = \frac{1}{\bar{r}''} - \frac{1}{\bar{r}'} + \frac{1}{RT}(\bar{\bar{G}}^{E'} - \bar{\bar{G}}^{E''}) + (1 - \psi_B') \frac{\partial \bar{\bar{G}}^{E'}/RT}{\partial \psi_B'} - (1 - \psi_B'') \frac{\partial \bar{\bar{G}}^{E'}/RT}{\partial \psi_B''} + \frac{\tilde{Y}_B''}{\psi_B''} \frac{\partial \bar{\bar{G}}^{E''}/RT}{\partial \tilde{Y}_B''} - \frac{\tilde{Y}_B'}{\psi_B'} \frac{\partial \bar{\bar{G}}^{E'}/RT}{\partial \tilde{Y}_B'}, \tag{30a}$$

$$B_B = \frac{1}{\psi_B'} \frac{\partial \bar{\bar{G}}^{E'}/RT}{\partial \tilde{Y}_B'} - \frac{1}{\psi_B''} \frac{\partial \bar{\bar{G}}^{E''}/RT}{\partial \tilde{Y}_B''}. \tag{30b}$$

These relations follow from the definitions of ρ_B (Eq. 9c) and of $\ln \bar{\bar{f}}_B$ (Eq. 19a). The equations for A_C amd B_C, resulting from Eqs. (9d) and (19b), read analogously.

The six unknowns on the left-hand sides of Eqs. (26)-(28) represent the solution of a system of nonlinear equations to be treated by numerical methods. Because of $\psi_B'' + \psi_C'' = 1$, one of the equations can be used for the determination of the equilibrium temperature T (or of the corresponding value of $\beta(T)$). For performing the calculations by a computer program,

the system may be reduced to four equations (Eqs. 27 and 28). The quantities $\bar{r}_B''$ and $\bar{r}_C''$ can be directly inserted into these four equations according to Eqs. (26a) and (26b).

RESULTS AND DISCUSSION

As a first step, mainly the influences of both polydispersities and of the various parameters included in the $\bar{\bar{G}}^E$ model will be discussed. Thus, calculations are performed by using model mixtures for the copolymer system B + C. Examples for real systems are chosen for demonstration purposes and do not represent the results of detailed and sophisticated analysis of the phase behavior of the blends concerned.

1. Blends of the Type B($\alpha\beta$) + C($\alpha\beta$)

It is known that two random copolymers, composed of the same two monomers α and β but differing in chemical composition $\tilde{Y}_B$ and $\tilde{Y}_C$, may be miscible under conditions of T and P where the two homopolymers are only partially miscible [17]. The theoretical result given by Scott [4] states that, at given T and P, the maximum deviation $\Delta_{max} = \tilde{Y}_C - \tilde{Y}_B$ that is allowed for a compatible mixture will be independent of the mean $(\tilde{Y}_B + \tilde{Y}_C)/2$ if the concentration of the mixture and the molecular weights of B and C are fixed. Using the spinodal equation and the critical-point condition in the binary system B($\alpha\beta$) + C($\alpha\beta$) of monodisperse copolymers, Casper and Morbitzer [18] gave a quite detailed study of the stability limits of such compatible mixtures. Also, on the basis of the spinodal and the critical point only, Koningsveld et al. showed that deviations from the "constant-Δ rule" may be due to polydispersity effects [7] or to surface/volume differences of the comonomers α and β [8].

In this section the problem will be discussed on the basis of the cloud-point and shadow curves, the true envelopes of the demixing region. Model calculations are carried out for the following conditions:

1. $\bar{r}_B' = 50$, $k_B = 1$, $\bar{r}_C' = 50$, $k_C = 1$, all $s_i = 1$, $\Delta = \tilde{Y}_C' - \tilde{Y}_B' = 0.1$ = constant $g_{\alpha\beta} = 1$.
2. Parameters as for 1, but Δ increases.
3. Parameters as for 1, but $\Delta = 0.2$ and ϵ_C increases.
4. Parameters as for 3, but ϵ_C = constant and s_β/s_α increases.
5. Parameters as for 4, but $s_\beta/s_\alpha = 1$ and k_C increases.
6. Parameters as for 5, but $k_C = 1$ and $\bar{\bar{G}}^E$ parameters c and $d \neq 0$.

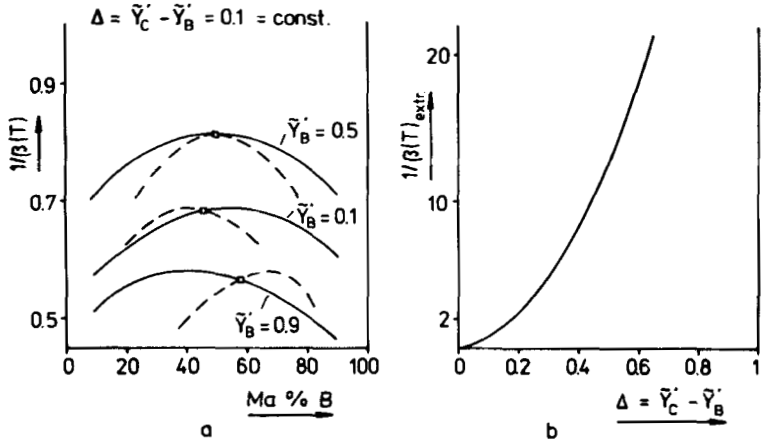

FIG. 1. Calculated phase equilibria in copolymer blends of the type B($\alpha\beta$) + C($\alpha\beta$). Note: ma% ≡ wt%.) (a) Cloud-point curves (—), shadow curves (- -), and critical points (□), $\bar{r}_B' = \bar{r}_C' = 50$, $k_B = k_C = 1$, all $s_i = 1$. (b) Extremum of the cloud-point curve versus $\Delta = \tilde{Y}_C' - \tilde{Y}_B'$. Other parameters as in (a).

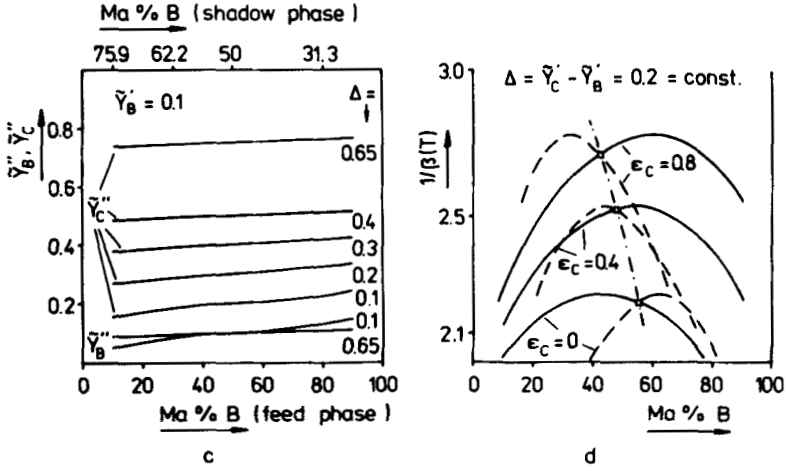

(c) Weight averages of the chemical composition, $\tilde{Y}_B''$ and $\tilde{Y}_C''$, in the shadow phase versus Δ. $\tilde{Y}_B' = 0.1$ = constant. Other parameters as in (a). (d) Cloud-point curves (—), shadow curves (- -), critical points (□), and critical line (—•—) for different widths of the chemical distribution ϵ_C of C. $\tilde{Y}_B' = 0.3$, $\tilde{Y}_C' = 0.5$, $\epsilon_B = 0.21$. Other parameters as in (a).

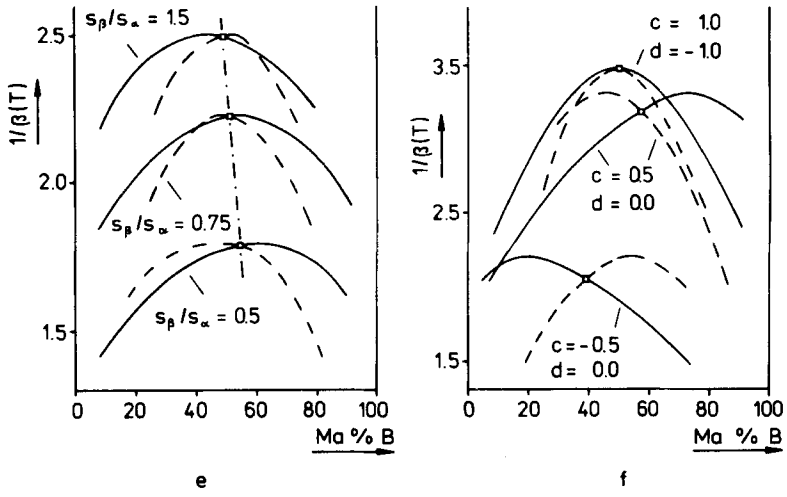

FIG. 1 (continued). (e) Cloud-point curves (—), shadow curves (- -), critical points (□), and critical line (— • —) for several ratios $s\beta/s_\alpha$. $\tilde{Y}_B' = 0.3$, $\tilde{Y}c = 0.5$. Other parameters as in (a). (f) Cloud-point curves (—), shadow curves (- -), and critical points (□) for different pairs of c and d parameters in $L(\psi_B)$. Other parameters as in (c).

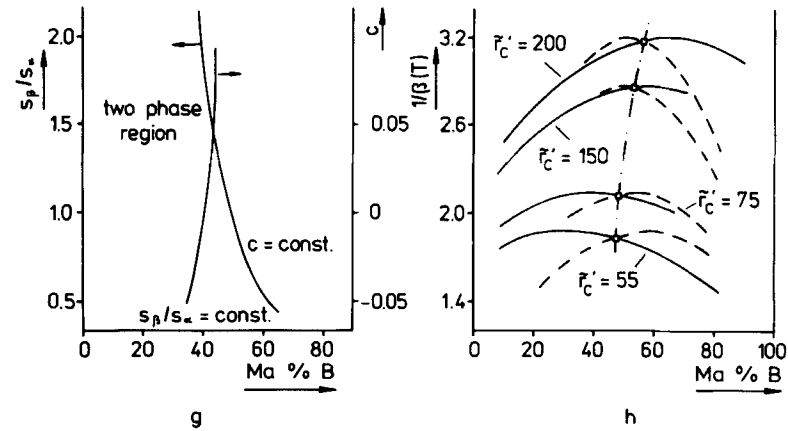

(g) Threshold concentration (at $1/\beta(T)_{extr}$) versus $s\beta/s_\alpha$, and versus the c parameter of $L(\psi_B)$. Other parameters as in (c). (h) Cloud-point curves (—), shadow curves (- -), critical points (□), and critical line (— • —) for several widths of the chain-length distribution of C. $s\beta/s_\alpha = 1$. Other parameters as in (c).

The characteristic results, summarized in Figs. 1a-h, lead to the following conclusions. The choice of $g_{\alpha\beta}$ is arbitrary in the presence of only two monomer units, α and β, because $g_{\alpha\beta} = g_{\beta\alpha}$. The function $\beta(T)$ is a solution of the phase equilibrium calculation, the order of $\beta(T)$ is given by the choice of $\bar{r}_B$ and $\bar{r}_C$ and, finally, $\beta(T)$ has to be adjusted to the experimental cloud-point curve in practical cases. Therefore, $g_{\alpha\beta} = 1$ is used in all cases discussed here.

Comparison of the different factors influencing the cloud-point curve reveals that the main effect is caused by the difference of chemical compositions $\Delta = \tilde{Y}_C' - \tilde{Y}_B'$ (see Figs. 1d-f, h), as had been found earlier for the monodisperse case [4]. Nevertheless, there are distinct effects on the exact location of the phase boundary keeping $\Delta = \tilde{Y}_C' - \tilde{Y}_B'$ constant. Figure 1(a) demonstrates that chemical polydispersity leads to a shift of the extremum of the cloud-point curve (the threshold value) and of the critical point. For Copolymer B(α,β), with $\tilde{Y}_B' = 0.9$, plus homopolymer C(α), with $\tilde{Y}_C = 1$, the extremum is located at about 40 mass percent (ma% ≡ wt%) B and the critical point at about 57 ma% B.

Keeping $\Delta = 0.1$ constant and decreasing $\tilde{Y}_B'$, the threshold leads to an extremum in $1/\beta(T)$, i.e., in temperature, if ϵ_B or ϵ_C possess their maximum of 0.25. After a further decrease of $\tilde{Y}_B'$ to the case of Homopolymer B(β), with $\tilde{Y}_B' = 0$, plus Copolymer C($\alpha\beta$), with $\tilde{Y}_C' = 0.1$, the symmetrical case (because of $\bar{r}_B' = \bar{r}_C'$, $k_B = k_C$) to $\tilde{Y}_B' = 0.9$ and $\tilde{Y}_C' = 1$ occurs with the extremum in $1/\beta(T)$ at about 60 ma% B and the critical point at about 43 ma% B. To sharpen this effect, caused mainly by the width of the chemical distribution, Fig. 1(d) shows how an increase in ϵ_C (not using Eq. 5b for ϵ_C) changes the main features of the phase diagram. Starting with a chemical monodisperse Copolymer C (as in nearly all cases considered in the literature) and increasing ϵ_C again shifts the critical point and the threshold concentration.

The critical point moves from the right-hand shoulder to the left-hand side in comparison to the extremum. Of course, this is a model calculation, but it makes clear how large the influence of the chemical distribution may become. The fractionation effect regarding the chemical distribution, Fig. 1(c), is comparatively small. It can be seen that $\Delta'' = \tilde{Y}_C'' - \tilde{Y}_B''$ is approximately constant and that Δ'' does not differ much from the initial value in the homogeneous phase. $\tilde{Y}_B''$ and $\tilde{Y}_C''$ are not strictly parallel, but this is almost beyond the possible accuracy of the lines drawn in Fig. 1(c).

The change in $\tilde{Y}_B''$ and $\tilde{Y}_C''$ is far less than the ordinary fractionation effect in $\bar{r}_B''$ and $\bar{r}_C''$. This is certainly due to the assumed random character of the copolymers and the Gaussian form of the chemical distribution. As a result of Eq. (28), all factors that possibly influence $\tilde{Y}_B''$ and $\tilde{Y}_C''$ have

to appear in the terms B_B and B_C, which also depend on Δ, but these terms turn out to be small. As already pointed out by Koningsveld et al. [7-9] on the basis of their spinodal analysis, changes of the surface ratio s_β/s_α (Fig. 1e) and of the width of the chain-length distribution (Fig. 1h) lead to certain shifts of the phase boundary, of its extremum, and of the critical point. Furthermore, the same effects can be observed by introducing the concentration-dependent term $L(\psi_B)$ in $\bar{\bar{G}}^E$ (Eq. 17). As Fig. 1(g) demonstrates, these effects may compensate each other to some extent. This is also true for the location of the critical point on the left-hand side or on the right-hand side of the extremum of the cloud-point curve.

Figures 1a-h do not include any assumption whether lower or upper critical solution behavior is considered. This is mainly a question of the form of $1/\beta(T)$. But, of course, the correct location of the critical point and the extremum have to be taken into account when adjusting parameters like s_α, s_β, c, and d to experimental cloud-point curves. Figures 1a-h help to find the correct relations and tendencies.

Some practical aspects will be demonstrated by applying the results discussed to some systems that have been investigated experimentally. Schmitt et al. [19] reported some observations by neutron scattering on the compatibility of copoly(acrylonitrile)s characterized by different mean chemical compositions and found miscibility in a certain range of Δ and $\bar{r}$. Figure 2 presents some results obtained by using a standard segment with a molecular weight of 100, which is close to the segment size used by Schmitt [19]. As expected from Fig. 1(b), Δ is again the main factor for the location of the cloud-point curve. At a fixed value of $1/\beta(T)$, i.e., of temperature, a certain miscibility range can be constructed. Figure 2(b) shows the fair agreement of our calculations with the experimental results (taken from Fig. 3 in Ref. 19) for the width of the miscibility range with increasing $\bar{r}'$ of the mixed copolymers. The calculations are performed on the simplified basis $c = d = 0$ and $s_\beta/s_\alpha = 1$ because no phase diagram was given in Ref. 19.

An example of the case Homopolymer B(α) + Copolymer C(α,β) was discussed earlier [16]. Here some cloud-point curves for the system polyethylene + (ethylene-co-acetate) published by Druz et al. [20] will be analyzed. From their material the series polyethylene PE2, PE4, PE5, PE100 + poly(ethylene-*co*-vinyl acetate) EVA29 is chosen. The samples are characterized by PE2, $\bar{M}_n$ 2000; PE4, $\bar{M}_n$ 4000; PE5, $\bar{M}_n$ 5000; PE100, $\bar{M}_n$ 100 000; EVA29, $\bar{M}_n$ 15 500; vinyl acetate content 28.9 ma%. Because nothing is reported on $\bar{M}_w$, PE2, PE4, PE5, and EVA29 are assumed to show a ratio of $\bar{M}_w/\bar{M}_n = 2$ and PE100 of $\bar{M}_w/\bar{M}_n = 4$, which are reasonable numbers for such products. Of course, the true values of $\bar{M}_w$ will influence the actual results to some extent

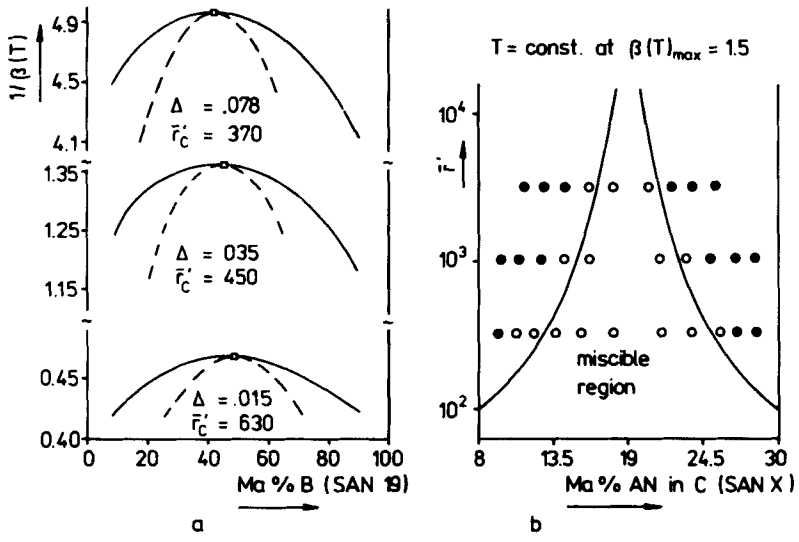

FIG. 2. Calculated phase equilibria in blends of two poly(styrene-*co*-acrylonitrile polymers (SAN). (a) Cloud-point curve (—), shadow curve (- -), and critical point (□) in blends of SAN 19 + SAN X (X = ma% of acrylonitrile). (b) Miscibility region for $\bar{r}_B = \bar{r}_C$ versus Δ in blends of SAN 19 + SAN X. Experimental points according to Ref. 19: (●) turbid, (○) transparent.

but not the general conclusions to be drawn. $M_S = 100$ is used, as above. The systems show upper critical solution behavior. The parameter c of $L(\psi_B)$ is adjusted to the experimental maximum of the system PE2 + EVA29. The results in Fig. 3(a) are calculated with the fitted value $c = 0.062$ and $s_\beta/s_\alpha = 1$. The experimental shifting of the maximum and the calculated results on maximum and critical point agree. To obtain full correspondence with the experimental cloud-point curves in the T-ψ_B plane, Fig. 3(b), the $\beta(T)$ function has to be adjusted for each single system. The result,

$$\text{PE2 + EVA29: } \beta(T) = -0.01013 + 121.844K/T,$$

$$\text{PE4 + EVA29: } \beta(T) = -0.05639 + 99.324K/T,$$

$$\text{PE5 + EVA29: } \beta(T) = -0.06185 + 93.566K/T,$$

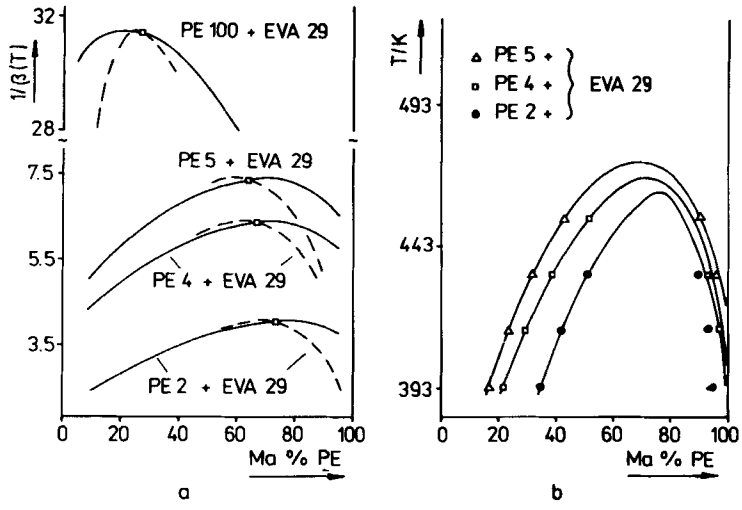

FIG. 3. Calculated phase equilibria in blends of polyethylene and poly-(ethylene-*co*-vinyl acetate). (a) Cloud-point curves (—), shadow curves (- -), and critical points (□) calculated on the basis of equal $\beta(T)$ functions. See text for parameters. (b) Cloud-point curves (—) for the same mixtures as in (a) but with fitted $\beta(T)$ functions. Experimental values from Ref. 20. See text for explanation.

demonstrates a certain dependence of $\bar{\bar{G}}^E$ on $\bar{M}_n$, which was not taken into account in the model used. The system PE100 + EVA29 lies beyond this picture and is not shown in Fig. 3(b). The results of Ref. 20 show a much too small difference between the demixing curves of PE5 + EVA29 and PE100 + EVA29, according to our calculations.

2. Blends of the Type B($\alpha\beta$) + C(γ)

There is experimental (e.g., Refs. 1, 17, 21, and 22) and theoretical (e.g., Refs. 2, 3, 5, 6, and 8) evidence that blends composed of a copolymer and a homopolymer formed by different monomer units may be compatible even if the homopolymer mixtures ($\alpha + \gamma$ or $\beta + \gamma$) are incompatible. This can occur in the absence of any specific interactions due to the so-called repulsion effect [2, 3], where the repulsion between the copolymer units α and β itself exceeds

the repulsion between each copolymer unit, α or β, and the homopolymer unit γ.

The so-called window of miscibility is observed when the phase behavior, which in most cases is of the lower critical solution temperature type, is plotted in a temperature versus copolymer composition (T vs $\tilde{Y}_B$) diagram. The most extensive experimental investigation of such blends, especially mixtures of copolymers from halogenated styrenes with poly(dimethylphenylene oxide), has been performed by Karasz and coworkers, who have published about 20 papers on these systems starting with Ref. 22. Theoretical discussion (e.g., Refs. 2, 3, 5, 6, and 18) is limited in most cases to the analysis of spinodal and the critical point in binary (i.e., monodisperse) mixtures, and sometimes the stability is even deduced from the negative sign of $\Delta_M G$ or $\bar{\bar{G}}^E$, as in Case 1 discussed above. To our knowledge, there is no paper that takes chain length and chemical distributions explicitly into account. This is so also for calculated phase diagrams in the literature.

Again, the starting point will be model calculations for cloud-point curves in B($\alpha\beta$) + C(γ) systems. However, compared to the case B($\alpha\beta$) + C($\alpha\beta$), there is now a much more complicated situation. First of all, some arguments regarding the values of $g_{\alpha\beta}$, $g_{\alpha\gamma}$, and $g_{\beta\gamma}$ are needed. With emphasis on the polydispersity effects, the parameter relations given by Kammer [5] are used. The model mixture is given by the same initial values as for Case 1 of B($\alpha\beta$) + C($\alpha\beta$), which permits comparison of some effects in this former case.

After assuming again $\bar{r}_B' = \bar{r}_C' = 50$ and $k_B = k_C = 1$, the quantity $\tilde{Y}_B'$ is varied, while $\tilde{Y}_C = 1$. Figures 4(a)-4(d) give insight into some of the main features. The expected results are obtained by variation of $\tilde{Y}_B'$, i.e., the miscibility window (Fig. 4b) or the division of the $1/\beta(T)$ versus $\tilde{Y}_B'$ diagram into a compatible and an incompatible region, depending on whether or not the attraction is larger than the repulsion (Fig. 4c). The influence of both chemical and molecular weight distribution is of the same order as in the case B($\alpha\beta$) + C($\alpha\beta$). Figure 4(a) shows the splitting of the phase diagram into cloud-point curve and shadow curve. Because $\tilde{Y}_C = 1$, fractionation with regard to the chemical composition occurs only with Copolymer B, and the curves of $\tilde{Y}_B''$ versus ψ_B look like those in Fig. 1(c) and are not reproduced here. Again, the fractionation effect for $\bar{r}_i''$ is much larger than for $\tilde{Y}_B''$. Variation of k_B or k_C leads to the same effects as in Fig. 1(h). There is a certain shift in the curves in Figs. 4(b) and 4(c) when the width of the chain-length distribution, i.e., k_B and k_C, is varied. As shown in Figs. 1(d)-1(f) and 1(h), all these effects can act in the same direction or can balance each other when combined properly. This behavior is demonstrated by variation of s_i (Fig. 1d), but the curves look alike when the c and d parameters, or ϵ_B at constant $\tilde{Y}_B'$, or k_B and k_C are varied in certain ways.

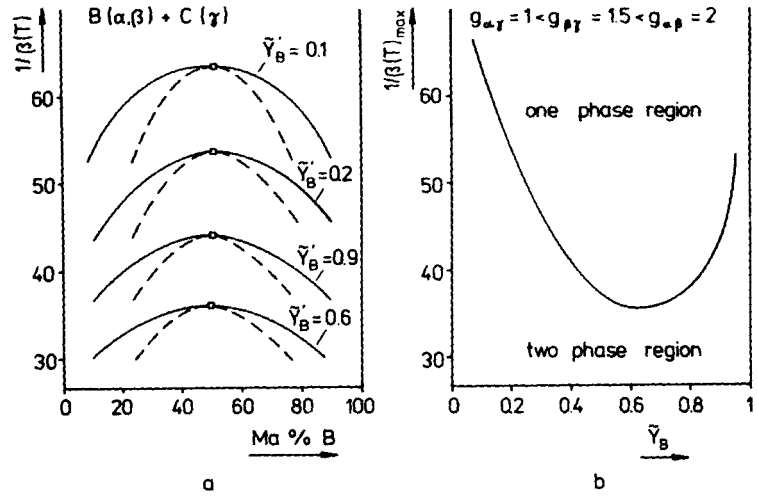

FIG. 4. Calculated phase equilibria in copolymer blends of the type B($\alpha\beta$) + C(γ). (a) Cloud-point curves (—), shadow curves (- -), and critical points (□) for different $\tilde{Y}_B{}'$ (α content in B). $\bar{r}_B{}' = \bar{r}_C{}' = 50$, $k_B = k_C = 1$, all $s_i = 1$, g_{ij} as in (b). (b) Window of miscibility formed by the mixtures of (a).

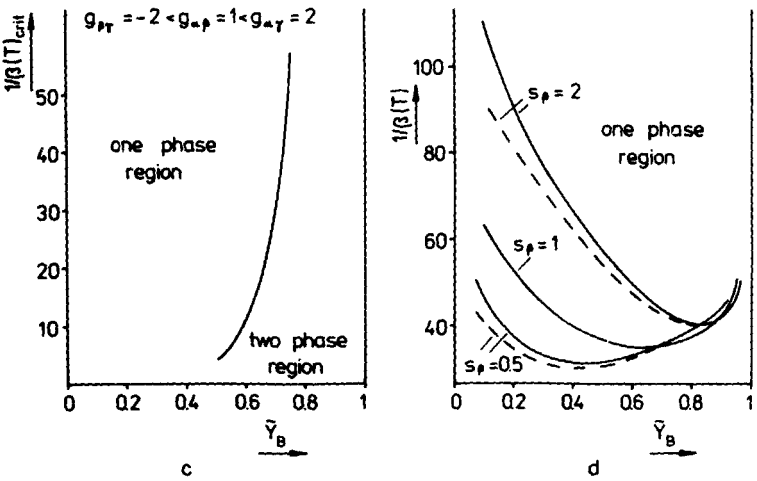

(c) The window of miscibility becomes a limit of miscibility by variation of the g_{ij} parameters. Other parameters as in (a). (d) Variation of the window of miscibility by variation of s_β: (- -) from critical point, (—) from extremum. $s_\alpha = s_\gamma = 1$. Other parameters as in (a).

The system poly(styrene-*co*-acrylonitrile) + poly(methyl methacrylate) was chosen as a real example. Stein et al. [23] reported compatibility in the range of 9 to 26.5 ma% of acrylonitrile in the copolymer. However, Schmitt [24] showed that, for certain acrylonitrile contents near 26 ma%, a very complicated phase behavior occurs characterized by two lower critical solution temperature ranges and additionally one upper critical solution temperature region. Kleintjens [25] presented a solution of the spinodal problem for this case by using the mean-field lattice-gas model and adjusting the surface/volume parameters to this diagram.

Putting this problem aside for the moment, as a first step the calculations will be applied to some cloud-point curves published recently by Kammer and coworkers [21]. Poly(methyl methacrylate) of $\bar{M}_w$ 43 000 and $\bar{M}_n$ 25 000 is mixed with a series of various poly(styrene-*co*-acrylonitrile)s with acrylonitrile contents of 9-35 ma%. As an example, the poly(styrene-*co*-acrylonitrile) sample is chosen for the calculations with $\bar{M}_w$ 179 000, $\bar{M}_n$ 91 000, and an acrylonitrile content of 34.4 ma%. The monomer units are defined by $\alpha = CH_2-CH-C_6H_5$, $\beta = CH_2-CH-CN$, and $\gamma = CH_2-C(CH_3)-COOCH_3$. The surface parameters are taken from the revised UNIFAC tables [26] and lead to $s_\beta/s_\alpha = 0.5$ and $s_\gamma/s_\alpha = 1.15$ as approximate values.

The more difficult problem is the estimation of the ratios $g_{\alpha\gamma}/g_{\alpha\beta}$ and $g_{\beta\gamma}/g_{\alpha\beta}$. The most suitable way would be to use phase-equilibrium data for the blends $\alpha\beta$, $\alpha\gamma$, and $\beta\gamma$ and to fit the g_{ij} parameters to the corresponding cloud-point curves. However, such experimental data are not available. Interaction parameters between polystyrene and poly(methyl methacrylate) in solutions of both copolymers were estimated by light scattering [27, 28] and from the liquid-liquid equilibrium in toluene [29-31]. Interaction parameters between α-units and β-units can be taken from the data published by Schmitt et al. [19] and our calculations above. There is no information on the interaction parameter between poly(acrylonitrile) and poly(methyl methacrylate). The ratio $g_{\alpha\gamma}/g_{\alpha\beta}$ is approximated on this basis to be about 1/2. The ratio of $g_{\beta\gamma}/g_{\alpha\beta}$ was chosen to be approximately 3/4 from the experience with model calculations (Fig. 4) with regard to the location of the miscibility window in agreement with the experimental findings [21]. Then the parameters c and d of $L(\psi_B)$ (Eq. 17) were adjusted to the minimum of the experimental cloud-point curve. As can be seen from Fig. 5(a), this results in $c = 0.3$ and $d = 0$ when the s_i-parameters are neglected. Readjusting c and d with $s_\beta/s_\alpha = 0.5$ and $s_\gamma/s_\alpha = 1.15$ leads to $c = -0.21$. Nevertheless, Fig. 5(b) demonstrates that both param-

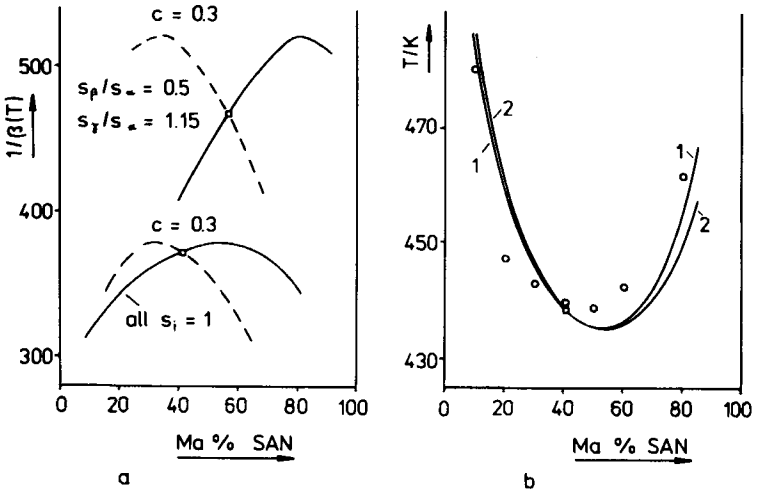

FIG. 5. Phase equilibria in blends of poly(styrene-*co*-acrylonitrile) (SAN) and poly(methyl methacrylate) (PMMA). (a) Cloud-point curve (—), shadow curve (- -), and critical point (□) in the system with SAN 34.4 for different ratios of the s values. For other parameters, see text. (b) Comparison of calculated and experimental results [29]. (□) Calculated critical point. 1: All $s_i = 1$, $c = 0.3$. 2: $s\beta/s\alpha = 0.5$, $s\beta/s\alpha = 1.15$, $c = -0.21$.

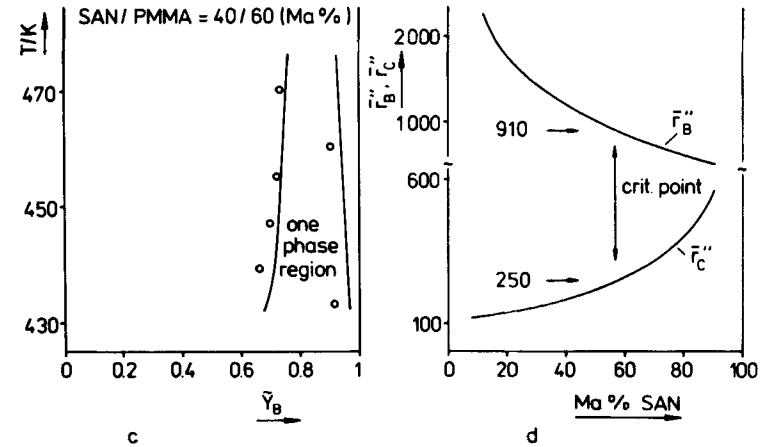

(c) Window of miscibility calculated with the parameters of Set 2 in (b). (○) Experimental results [21] for 40 ma% SAN in the blend. (d) Fractionation effect with respect to the mean segment numbers $\bar{r}''$. Parameters from (a) with $s_i \neq 1$.

eter sets work equally well when compared with the experimental data. The results of fitting the $\beta(T)$ function to them are $\beta(T) = 0.0080 - 2.33215K/T$ with $c = 0.3$ and $s_i = 1$, and $\beta(T) = 0.0067 - 1.7540K/T$ with $c = -0.21$ and s_i as indicated when $\bar{r}_B$ and $\bar{r}_C$ are obtained from $\bar{M}_n$ by division by $M_s = 100$.

Figure 5(c) shows the resulting miscibility window if all parameters are kept constant ($c = -0.21$, etc.) and $\tilde{Y}_B$ is varied. The right-hand side at $\tilde{Y}_B > 0.9$ is less accurate than the other side of the window. Figure 5(d) illustrates the fractionation effect with regard to the segment number (molecular weight, chain length), which is much stronger than the fractionation effect with respect to chemical composition. $\tilde{Y}_B''$ is a nearly linear function with a rather low slope of less than 0.3% of that of $\tilde{Y}_B'$.

3. Blends of the Type B(αβ) + C(γδ)

Matters are most complicated in this case, because there are six g_{ij} parameters, four s_i parameters, and the quantities $\tilde{Y}_B$, $\tilde{Y}_C$, $\bar{r}_B$, and $\bar{r}_C$ which may be varied. Some theoretical discussions regarding the g_{ij} parameters have been reported [1, 3, 5, 32] on the basis of the spinodal equation or of the negative sign of $\Delta_M G$. Our model calculations were again performed with the system $\bar{r}_B' = \bar{r}_C' = 50$, $k_B = k_C = 1$ to maintain comparability with the above results. Figures 6(a)-6(f) summarize some of the results obtained by com-

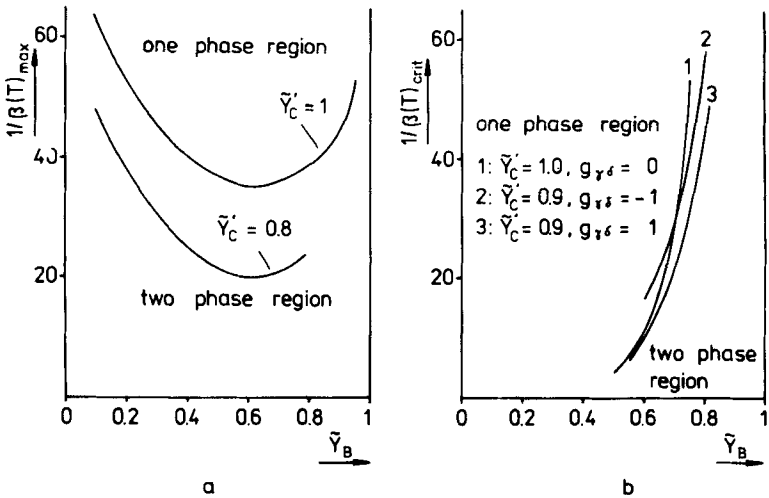

FIG. 6. Calculated phase equilibria in copolymer blends of the type B(αβ) + C(γδ). (a) Window of miscibility obtained with $g_{\alpha\gamma} = g_{\alpha\delta} = 1 < g_{\beta\gamma} = g_{\beta\delta} = 1.5 < g_{\alpha\beta} = g_{\gamma\delta} = 2$; $\bar{r}_B' = \bar{r}_C' = 50$, $k_B = k_C = 1$, all $s_i = 1$. (b) Limit of miscibility obtained with $g_{\beta\gamma} = g_{\beta\delta} = -2 < g_{\alpha\beta} = g_{\gamma\delta} = 0; \pm 1 < g_{\alpha\gamma} = g_{\alpha\delta} = 2$. Other parameters as in (a).

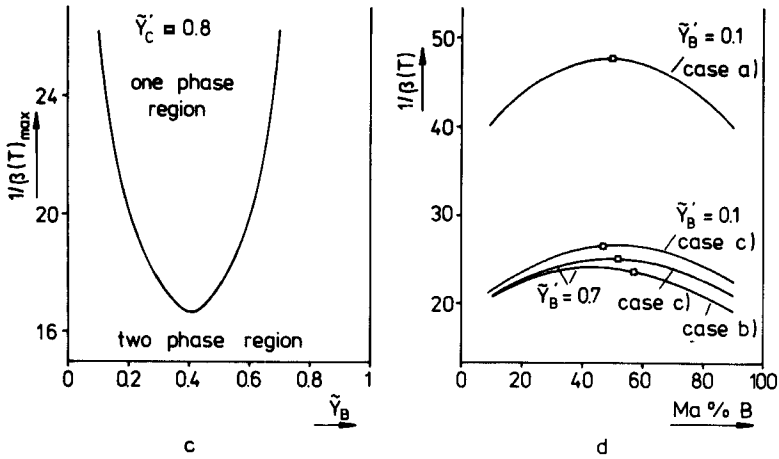

FIG. 6. (continued). (c) Window of miscibility obtained by combination of g_{ij} parameters from (a) and (b) with $g_{\alpha\gamma} = 1$, $g_{\beta\gamma} = 1.5$, $g_{\alpha\beta} = 2$, $g_{\beta\delta} = -2$, $g_{\gamma\delta} = 1$, $g_{\alpha\delta} = 2$. (d) Comparison of cloud-point curves (—) and critical points (□) for systems of (a), (b), and (c) with $\tilde{Y}_C' = 0.8$.

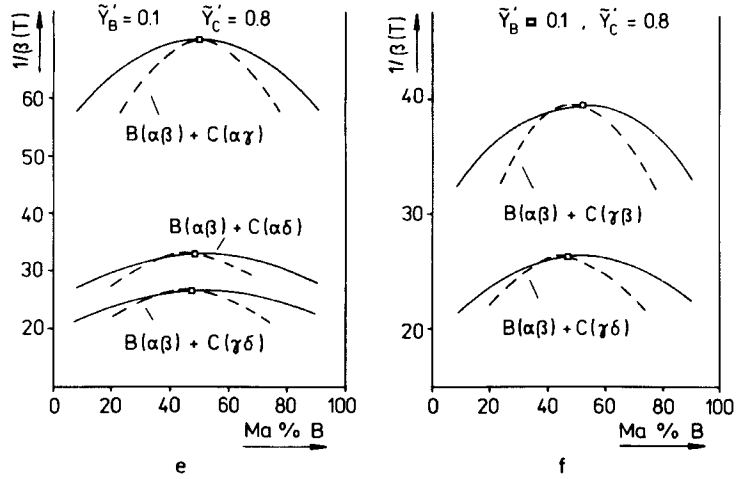

(e) Cloud-point curves (—), shadow curves (- -), and critical points (□) in blends with monomer unit α substituted for γ or δ in C. For parameters, see (c) and text. (f) Cloud-point curves (—), shadow curves (- -), and critical points (□) in blends with monomer unit β substituted for γ or δ in C. For parameters, see (c) and text. (B($\alpha\beta$) + C($\delta\beta$) is completely miscible under the given conditions.)

bining two g_{ij} parameter sets previously used for the case B($\alpha\beta$) + C(γ). Thus all possible influencing factors are restricted to one question only: How will a fourth copolymer unit change the phase diagrams obtained before? Suppose $g_{\alpha\delta} = g_{\alpha\gamma}, g_{\beta\delta} = g_{\beta\gamma}$, and $g_{\gamma\delta} = g_{\alpha\beta}$ diagrams symmetrical to Figs. 4(b) and 4(c) are obtained, resulting in a shift of the miscibility window to lower $1/\beta(T)$ values, i.e., the compatibility region becomes larger (Fig. 6a). By taking attractive forces ($g_{ij} < 0$) into account, diagrams resembling the behavior of Fig. 4(c) are observed (Fig. 6b), but a miscibility window may also be found (Fig. 6c). Upon comparing the cloud-point curves belonging to Figs. 6(b) and 6(c), smaller differences (see the lower three curves in Fig. 6c) than would be expected are seen.

Finally, it would be interesting to see how the phase diagrams will change if one of the two units (γ, δ) in Copolymer C is replaced by a monomer unit α or β from Copolymer B. Figures 6(e) and 6(f) give the results obtained for such "subsystems." The most drastic effects for the parameter combination of Fig. 4(c) are observed if the monomer unit δ is replaced by the monomer unit α (i.e., $g_{\alpha\delta} = 0, g_{\gamma\delta} = g_{\alpha\gamma}, g_{\beta\delta} = g_{\alpha\beta}$), which is mainly due to the change of the attractive value $g_{\beta\delta} = -2$ from Fig. 4(c) to the repulsive value $g_{\alpha\beta} = +2$. On the other hand (Fig. 6f), complete miscibility is calculated ($\beta(T) < 0$) if unit γ is replaced by unit β (i.e., $g_{\beta\gamma} = 0$, $g_{\gamma\delta} = g_{\beta\delta}, g_{\alpha\gamma} = g_{\alpha\beta}$, and $g_{\gamma\delta}$ changes from +1 to -2). There are many more possible combinations leading to compatibility or to certain phase diagrams which cannot all be outlined here.

This paper concludes by considering a practical example of the case B($\alpha\beta$) + C($\gamma\beta$). Unfortunately, only a very small number of corresponding phase diagrams can be found in the literature (see Refs. 1 and 17 for primary references). Thus, our calculations shall be applied to the system B poly(styrene-*co*-acrylonitrile) + C (butadiene-*co*-acrylonitrile) recently investigated by Ougizawa and Inoue [32]. Both copolymers can be assumed to be random products with the following properties. Poly(styrene-*co*-acrylonitrile): $\bar{M}_n$ 68 400, $\bar{M}_w$ 194 000, acrylonitrile content 25 ma%; poly(butadiene-*co*-acrylonitrile): $\bar{M}_n$ 91 300, $\bar{M}_w$ 297 000, acrylonitrile content 40 ma%.

Thus, there is an advantage if Copolymer B is the same product as was used in the examples above. Reliable information on the interaction parameter $g_{\alpha\gamma}$ of polystyrene with polybutadiene can be taken from Ref. 33. Cloud-point curves of poly(styrene-*co*-butadiene) with its parent homopolymers are given in Ref. 34. Nothing could be found on the interaction between polybutadiene and polyacrylonitrile. The units α and β are defined as above, and γ by CH_2–CH=CH–CH_2 (assuming an atactic product). The ratios s_i/s_α, again obtained from the surface parameters [26], are $s_\beta/s_\alpha = 0.5$ and $s_\gamma/s_\alpha = 0.6$. The g_{ij} parameters were estimated by using the infor-

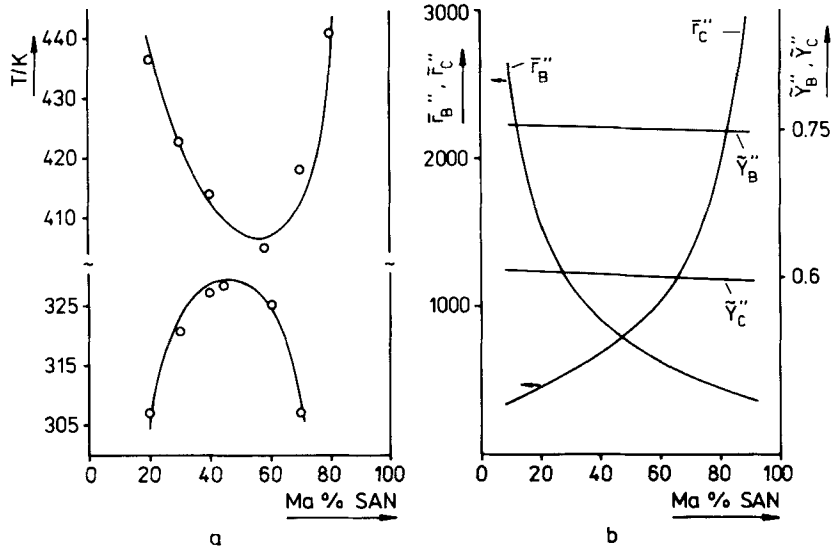

FIG. 7. Phase equilibria in blends of poly(styrene-*co*-acrylonitrile) (SAN) and poly(styrene-*co*-butadiene) (SB). (a) Calculated cloud-point curves (—) in comparison with experimental results [32]. See text for parameters. (b) Fractionation effects with respect to $\bar{r}''$ and $\tilde{Y}''$ for the case of lower critical solution temperature in (a).

mation from Refs. 32 and 33 and from the results obtained above, leading to $g_{\alpha\gamma}/g_{\alpha\beta} = 0.05$ and $g_{\beta\gamma}/g_{\alpha\beta} = 1.45$. The parameters c and d in $L(\psi_B)$ were adjusted to the minimum or maximum, respectively, of the demixing curves given in Ref. 32. The two parameter sets for c and d are somewhat different because both extrema do not occur at the same blend composition. Figure 7 shows the final result, where the upper curve is calculated with $c = 0.55$, $d = 0$, and $\beta(T) = 0.20392 - 49.3461K/T$ for lower critical solution temperature behavior; and the lower curve, exhibiting upper critical solution temperature behavior, is obtained with $c = 0.38$, $d = 0.01$, and $\beta(T) = 0.039595 + 16.87692\ K/T$. Again, the fractionation effect influences $\bar{r}''$ primarily and $\tilde{Y}''$ less (Fig. 7b).

CONCLUDING REMARKS

The aim of this paper was to apply continuous thermodynamics to the liquid-liquid equilibrium in blends of random copolymers that are polydisperse both in

molecular weight and chemical composition. The generalized Stockmayer distribution (Eq. 4) was used to obtain analytical solutions of the occurring double integrals, and one has to be aware that this choice may influence the results of the model calculations. Three general cases were considered to some extent. The influences of various model parameters were discussed with respect to the resulting phase diagrams. Emphasis was placed on the fact that all conclusions were drawn here on the basis of the true envelope of the demixing region in polydisperse systems (the so-called cloud-point curve) instead of using the limit of instability (spinodal) or only the sign of $\Delta_M G$, as is usually done in the literature. Comparison with some experimental results showed acceptable results, notwithstanding a certain number of assumptions necessary for the practical calculations. The neglect of both polydispersities leads to a distinct loss in understanding of liquid-liquid phenomena in copolymer blends.

REFERENCES

[1] R.-J. Roe and D. Rigby, *Adv. Polym. Sci., 82,* 105 (1987).
[2] G. ten Brinke F. E. Karasz, and W. J. MacKnight, *Macromolecules, 16,* 1827 (1983).
[3] D. R. Paul and J. W. Barlow, *Polymer, 25,* 487 (1984).
[4] R. L. Scott, *J. Polym. Sci., 9,* 423 (1952).
[5] H. W. Kammer, *Acta Polym., 37,* 1 (1986).
[6] C. G. Panayiotou, *Makromol. Chem., 188,* 2733 (1987).
[7] R. Koningsveld and L. A. Kleintjens, *J. Polym. Sci., Polym. Symp., 61,* 221 (1977).
[8] R. Koningsveld, L. A. Kleintjens, and G. Markert, *Macromolecules, 10,* 1105 (1977).
[9] R. Koningsveld and L. A. Kleintjens, *Macromolecules, 18,* 243 (1985).
[10] M. T. Rätzsch and H. Kehlen, *J. Macromol. Sci.–Chem., A22,* 323 (1985).
[11] M. T. Rätzsch, H. Kehlen, and J. Bergmann, *Z. Phys. Chem. (Leipzig), 264,* 318 (1983).
[12] H. Kehlen, M. T. Rätzsch, and D. Thieme, *J. Macromol. Sci.–Chem., A23,* 811 (1986).
[13] M. T. Rätzsch, H. Kehlen, and D. Browarzik, *Ibid., A22,* 1679 (1985).
[14] M. T. Rätzsch, H. Kehlen, D. Browarzik, and M. Schirutschke, *Ibid., A23,* 1349 (1986).
[15] M. T. Rätzsch, D. Browarzik, and H. Kehlen, *Ibid., A26,* 903 (1989).

[16] D. Browarzik, H. Kehlen, M. T. Rätzsch, and D. Thieme, *Acta Polym.*, *39*, 687 (1988)
[17] S. Krause, *J. Macromol. Sci., Rev. Macromol. Chem., C7*, 251 (1972).
[18] R. Casper and L. Morbitzer, *Angew. Makromol. Chem., 58/59*, 1 (1977).
[19] B. Schmitt, R. G. Kirste, and J. Jelenic, *Makromol. Chem., 181*, 1655 (1980).
[20] N. I. Druz, A. E. Chalych, and A. D. Aliev, *Vysokomol. Soedin., Ser. B, 29*, 101 (1987).
[21] M. Suess, J. Kressler, and H. W. Kammer, *Polymer, 28*, 957 (1987).
[22] P. Alexandrovich, F. E. Karasz, and W. J. MacKnight, *Ibid., 18*, 1022 (1978).
[23] D. J. Stein, R. H. Jung K. H. Illers, and H. Hendus, *Angew. Makromol. Chem., 36*, 89 (1974).
[24] B. Schmitt, *Angew. Chem., 91*, 286 (1979).
[25] L. A. Kleintjens, in *Integration of Fundamental Polymer Science and Engineering*, Elsevier, London, 1986, pp. 56-66.
[26] J. Gmehling, P. Rasmussen, and A. Fredenslund, *Ind. Eng. Chem., Process Des. Dev., 21*, 118 (1982).
[27] A. Kratochvil, D. Strakova, and Z. Tuzar, *Br. Polym. J., 9*, 217 (1987).
[28] A. C. Su and J. R. Fried, *Macromolecules, 19*, 1417 (1986).
[29] W. W. Y. Lau, C. M. Burns, and R. Y. M. Huang, *J. Appl. Polym. Sci., 29*, 1531 (1984).
[30] W. W. Y. Lau, C. M. Burns, and R. Y. M. Huang, *Ibid., 30*, 1187 (1985).
[31] W. W. Y. Lau, C. M. Burns, and R. Y. M. Huang, *Eur. Polym. J., 23*, 37 (1987).
[32] T. Ougizawa and T. Inoue, *Polym. J., 18*, 521 (1986).
[33] R.-J. Roe and W.-C. Zin, *Macromolecules, 13*, 1221 (1980).
[34] A. Rameau J.-P. Lingelser, and Y. Gallot, *Makromol. Chem., Rapid Commun., 3*, 413 (1982).

Received September 28, 1988